Articles

An ab Initio MO Study of Silver Triflate Complexation in [2.2.1]Cyclophane π-Prismands

Pauli Saarenketo,† Reijo Suontamo, and Kari Rissanen*

University of Jyväskylä, Department of Chemistry, P.O. Box 35, Survontie 9, FIN-40351, Jyväskylä, Finland

Received November 26, 2001

Ab initio Hartree−Fock and DFT MO calculations have been used to study the conformations of six [2.2.1]cyclophane π-prismands and the formation of their π-complexes with silver triflate ($AgSO_3CF_3$). The lowest energy cyclophane conformations and their silver triflate π-complexes have been calculated with HF/3-21G* and B3LYP/3-21G* levels of theory. The nature of bonding in silver triflate π-complexes has been studied with natural bond orbital analysis (NBO). Energies of the calculated cyclophanes and complexes, together with the formation energies of those complexes, have also been discussed. The results have been compared to available X-ray crystal structures and also to results of the previously published ab initio calculations of slightly larger [2.2.2]cyclophanes and their silver complexes. Calculated and experimental X-ray structures agreed reasonably well, given the rather small 3-21G* basis set. Changes in the bonding between the ligand and Ag^+ ion were observed, due to an enhanced bonding of the triflate moiety over the silver atom ion in the calculated models. In these complexes the silver ion is bonded to the cyclophane cavity by the bonds formed by σ donation and d−π* back-donation between the silver ion and the hydrocarbon skeleton resulting in variable bonding modes from η^1 to η^6 per aromatic ring depending on the ligand conformation. In this case the σ donation from the hydrocarbon to the silver ion is the main contribution to the metal−cyclophane bonding. Bonding of the silver ion to the present π-prismands relates by strength to a single moderately strong hydrogen bond and varies between 25 and 50 kJ/mol. Due to the smaller cavity, the more rigid hydrocarbon skeleton, and the presence of the triflate moiety [2.2.1]cyclophanes form different types of interactions with silver ion when compared to previously published [2.2.2]cyclophane π-prismand complexes with Ag^+ ion.

Introduction

Polycyclic aromatic hydrocarbons form complexes with metal ions such as Ag^+. The bonding in these kinds of π-complexes is due to an electron transfer between the aromatic moiety and the positively charged metal cation.[1,2] Vögtle et al.[3] showed that concave hydrocarbons are able to extract certain metal cations from an aqueous solution. The complexation selectivity of the hydrocarbon cyclophanes allows applications such as incorporation in ion-selective electrodes. A number of cyclophanes were tested as ionophores, and as a result the PVC−[2.2.2]paracyclophane membrane showed a remarkable selectivity toward silver against alkali-metal, alkaline-earth-metal, and thallium ions.[3]

The cyclophanes presented here are [2.2.1]*p*,*p*,*p*- (**1**), [2.2.1]*p*,*m*,*p*- (**2**), [2.2.1]*m*,*p*,*p*- (**3**), [2.2.1]*m*,*m*,*p*- (**4**), [2.2.1]*p*,*m*,*m*- (**5**), and [2.2.1]*m*,*m*,*m*-cyclophane (**6**), belonging to the family of [2.2.1]cyclophane π-prismands. They also show complexation potential toward metal ions.

The well-known [2.2.2]*p*,*p*,*p*-cyclophane (**7**) was prepared by Pierre et al.[4] They used the modified Wurtz condensation of *p*-xylylene chloride in the presence of a catalytic amount of tetraphenylethylene.[5] The open-chain compound was also obtained in the reaction. The complexation studies[4] showed that silver trifluoromethanesulfonate (silver triflate) and **7** form an extraordinarily stable 1:1 complex where the Ag^+ cation is located inside the cyclophane cavity consisting of the three

* To whom correspondence should be addressed. E-mail: kari.rissanen@jyu.fi.

† Present address: Juvantia Pharma Ltd., Lemminkäisenkatu 5, Pharmacity, FIN-20520 Turku, Finland. E-mail: pauli.saarenketo@juvantia.com.

(1) Atwood, J. L.; Davies, J. E. D.; MacNicol, D. D.; Vögtle, F. *Comprehensive Supramolecular Chemistry*; Pergamon: Oxford, U.K., 1996; Vol. 1.

(2) Vögtle, F.; Seel, C.; Windscheif, P.-M. *Comprehensive Supramolecular Chemistry*; Pergamon: Oxford, U.K., 1996; Vol. 2, p 211.

(3) Gross, J.; Harder, G.; Siepen, A.; Harren, J.; Vögtle, F.; Stephan, H.; Gloe, K.; Ahlers, B.; Cammann, K.; Rissanen, K. *Chem. Eur. J.* **1996**, *2*, 1585.

(4) Pierre, J.-L.; Baret, P.; Chautemps, P.; Armand, M. *J. Am. Chem. Soc.* **1981**, *103*, 2986.

(5) Tabushi, I.; Yamada, H.; Yoshida, Z.; Oda, R. *Tetrahedron* **1971**, *27*, 4845.

10.1021/om0110134 CCC: $22.00
Publication on Web 11/05/2002

aromatic rings. Owing to its spatial shape and the complexation ability of **7**, the name "π-prismand"[4] was proposed for such hydrocarbon cyclophanes. X-ray crystallographic studies by Boekelheide et al.[6] verified later that the silver ion in the **7**−silver triflate complex is located on the 3-fold axis, outside of the π-prismand cavity, of the original hydrocarbon. This structure facilitates a η^2 Ag−C interaction with one carbon−carbon double bond on each phenyl moiety, leading to an overall η^6 ($3 \times \eta^2$) π-bonding between the silver ion and **7**.

Boekelheide et al.[6] found that the gas-phase dimerization of benzocyclobutenes under a nitrogen stream was an efficient method for making dibenzocyclooctadienes. When benzo[1,2;4,5]dicyclobutene was used under similar conditions, [2$_4$](1,2,4,5)cyclophane was obtained. Increasing the concentration of benzo[1,2;4,5]-dicyclobutene in the hot zone of the pyrolysis tube finally produced [2$_6$](1,2,4,5)cyclophane (deltaphane), which would be an ideal π-prismand.[6]

We have reported the syntheses of [2.2.2]*m,p,p*- (**8**) and [2.2.2]*m,m,p*-cyclophane (**9**),[7,8] which are based on the cyclophane methodology where sulfide cyclization is done under high dilution followed by oxidation and sulfone pyrolysis.[9,10] The synthesis of [2.2.2]*m,m,m*-cyclophane (**10**) has not been successful yet. The X-ray structures of **8**− and **9**−silver triflate show π-bonding between the silver ion and cyclophane ligand similar to that in the **7**−silver triflate complex, despite the ring size reduction and conformational isomerism.[7,8] We have also reported the synthesis and X-ray structures of [2.2.1]*p,p,p*- (**1**) and [2.2.1]*m,p,p*-cyclophanes (**3**) and their silver triflate complexes.[11] The synthesis was done using the same cyclophane methodology as in the case of [2.2.2]cyclophanes. In this paper we have used these X-ray structures in comparison to the calculated results.

The silver ion complexation in [2.2.2]cyclophane π-prismands has also been studied with ab initio MO calculations in our previous paper.[12] The studies show that the complex formation with Ag^+ cation was exothermic for the whole [2.2.2]cyclophane family (**7**−**10**), thus suggesting that the [2.2.2]*m,m,m*-cyclophane−AgY complex might also be possible to prepare and that it should have a structure similar to that of the other π-prismand complexes. The NBO analyses[13] of the π complexes of cyclophanes **7**−**10** show a rather normal bonding−back-bonding behavior. In most of the known cases,[14,15] the bonding part involves mainly d−π* back-bonding. It was shown that in these cyclophane complexes, however, the σ bonding aspect is dominant. The strength of the bonding can be compared to that of hydrogen bonds, which are usually weak, typically 20−25 kJ/mol, but which can also have bond enthalpies of over 100 kJ/mol.[16]

Here we report ab initio Hartree−Fock and density functional theory MO calculations of [2.2.1]cyclophanes **1**−**6** and their π complexes with silver triflate. Calculations were performed in order to gain information about the bonding and the effect of a smaller cavity on the nature of bonding in these π-prismand−silver triflate complexes. The nonbonded contact distances between silver ion and the carbon atoms closest to it, as well as bond and torsion angles of the optimized conformations, are compared to X-ray diffraction structures when available. The bonding and behavior of the triflate moiety in calculated complexes and in X-ray structures are also discussed. The nature of bonding is studied using natural bond orbital analysis (NBO).[13] The energies of the calculated ligands and complexes, as well as the formation energies of these complexes, are also discussed.

Experimental Section

The preliminary structures for modeling the cyclohanes **1**−**6** were created with the Cerius^2 molecular modeling program.[17] Molecular mechanics and Compass force field was used to calculate the steric energies and to reach the energy-minimized structures. The most stable conformations of the free **1**−**6** were found using a systematic method in Cerius^2. Molecular dynamics simulations were performed for all found conformations at a temperature of 1000 K under the constant-energy and constant-volume ensemble (NVE).[18] Each simulation took 2 ps in 0.001 ps steps. During the dynamics simulation conformations were minimized after every 100th step using a quenched dynamics method in order to collect all possible conformations. Two conformations were found for **1**, three for **2** and **3**, six for **4**, five for **5**, and seven for **6**.

All 26 found conformations of the free **1**−**6** were fully optimized at the HF/STO-3G level of theory. On the basis of the HF/STO-3G energies, 2−3 conformations lowest in energy for each cyclophane were chosen. The chosen conformations were again optimized at the HF/3-21G* level of theory. Of these, only the lowest energy conformation of each cyclophane was used for the calculations of their silver triflate complexes. This restriction is supported by the rigidity of the present cyclophanes **1**−**6**, complexation-suitable conformations of the lowest energy cyclophanes, and (in practice) the large computational cost of the calculations of complexes including whole silver triflate moieties.

Preliminary complex structures were made by adding the silver triflate guest on different sides of the chosen cyclophanes, thus giving two conformations for each cyclophane, where silver triflate is complexed to the ligand cavity from different directions. The structures were then fully optimized at the HF/3-21G* level of theory. The NBO analysis[13] was carried out for the lowest energy conformation of each complex. For comparison of energies and geometries the HF/3-21G* optimized cyclophanes and complexes were also optimized using DFT MO calculations at the B3LYP/3-21G* level of theory. The effect of triflate on the position and bonding energy of the silver ion in π-prismand−silver triflate complexes was studied by optimizing two π-prismand−Ag^+ complexes at both HF/3-21G* and B3LYP/3-21G* levels of theory. The NBO

(6) Kang, H. C.; Hanson, A. W.; Eaton, B.; Boekelheide, V. *J. Am. Chem. Soc.* **1985**, *107*, 1979.
(7) Seppälä, T.; Wegelius, E.; Rissanen, K. *New J. Chem.* **1998**, *22*, 789.
(8) Lahtinen, T.; Wegelius, E.; Airola, K.; Kolehmainen, E.; Rissanen, K. *J. Prakt. Chem.* **1999**, *341*, 237.
(9) Laufenberg, S.; Feuerbacher, N.; Pischel, I.; Börsch, O.; Nieger, M.; Vögtle, F. *Liebigs Ann. Chem.* **1997**, 1901.
(10) Vögtle, F. *Cyclophane Chemistry*; Wiley: Chichester, U.K., 1993.
(11) Lahtinen, T.; Wegelius, E.; Rissanen, K. *New J. Chem.* **2001**, *25*, 905−911.
(12) Saarenketo, P.; Suontamo, R.; Jödicke, T.; Rissanen, K. *Organometallics* **2000**, *19*, 2346.
(13) Glendening, E. D.; Reed, A. E.; Carpenter, J. E.; Weinhold, F. NBO, version 3.1.
(14) Huang, H. Y.; Padin, J.; Yang, R. T. *J. Phys. Chem. B* **1999**, *103*, 3206.
(15) Kovács, A.; Frenking, G. *Organometallics* **1999**, *18*, 887.
(16) Shriver, D. F.; Atkins, P. W.; Langford, C. H. *Inorganic Chemistry*; Oxford University Press: Oxford, U.K., 1994.
(17) *Cerius^2 Conformational Search and Analysis*; Molecular Simulations: San Diego, CA, 1997.
(18) *Force field-Based Simulations General Theory & Methodology*; Molecular Simulations: San Diego, CA, 1997.

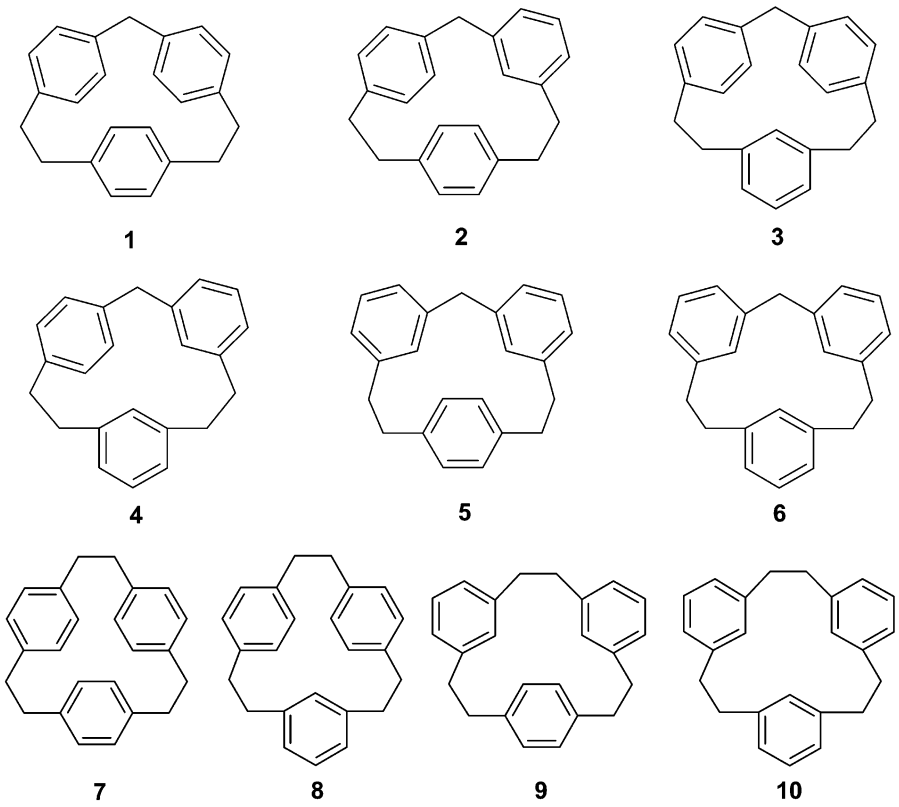

Figure 1. Cyclophanes **1**−**10**.

analysis was performed for these π-prismand−Ag^+ complexes during optimization and also for available X-ray structures during single-point calculations at the HF/3-21G* level of theory.

Natural bond orbital analysis is based on a method for optimally transforming a given wave function into a localized form, corresponding to the one-center ("lone pair") and two-center ("bond") elements of the chemist's Lewis structure. In the first step the input atomic orbital basis set is transformed into natural atomic orbitals (NAO). Natural charges on atoms, valencies, and overlap-corrected bond orders based on NAO electron populations provide estimates of the ionic and covalent components of the bonding and provide qualitative correlations with the bond distances.[13] Bond orders give estimates of the covalent bonding present so that a value of ∼1 corresponds to a single bond, a bond order value of ∼2 equals a double bond, etc.

All ab initio MO calculations were performed with the Gaussian 98 series of programs.[19] A modified GDIIS optimization algorithm for large systems and molecules with flat potential energy surfaces were used instead of the standard Berny algorithm due to convergence problems for optimization of the complexes.

The asymmetric unit of the X-ray structure of **1**−silver triflate[11] contained four complexes, from which one complex was selected for comparison against calculation results. Other X-ray structures used in this paper contain only one molecule or complex in their asymmetric units.

In this paper the results of HF and DFT calculations are compared to the results in our previous paper[12] obtained using the same basis set and method. Comparisons are done only for the values which are not dependent on the number of atoms present. The basis set superposition error (BSSE) has been taken into consideration by calculating counterpoise correction for complex formation energies.[20] This correction has also been applied to complex formation energy calculations of our previous paper,[12] and corrected results are presented here.

Results and Discussion

The Cyclophanes. The cyclophanes **1**−**6** (Figure 1) form a series of structurally isomeric compounds. They each have the same $C_{23}H_{22}$ skeleton, but the ring size is changed from the 17-membered ring of **1** to the 14-membered ring of **6**. The reduction of ring size is caused by the change of spatial connections inside the isomeric skeleton. The cavity inside **1**−**6** is smaller than in the cyclophanes **7**−**10** (Figure 1), which we have reported in our previous papers.[7,8,12] This has an effect on the complexation properties and bonding trends in the studied silver triflate cyclophane complexes.

The energies of the most stable conformations of **1**−**6** are shown in Table 1. The energy differences between the lowest energy conformations of different cyclophanes are similar to those between the conformations of one cyclophane. The energy cap between the lowest and the second lowest energy conformation is clearly smaller than the energy cap between the second and the third lowest conformation, except in the case of **6**. This trend

(19) Frisch, M. J.; Trucks, G. W.; Schlegel, H. B.; Scuseria, G. E.; Robb, M. A.; Cheeseman, J. R.; Zakrzewski, V. G.; Montgomery, J. A., Jr.; Stratmann, R. E.; Burant, J. C.; Dapprich, S.; Millam, J. M.; Daniels, A. D.; Kudin, K. N.; Strain, M. C.; Farkas, O.; Tomasi, J.; Barone, V.; Cossi, M.; Cammi, R.; Mennucci, B.; Pomelli, C.; Adamo, C.; Clifford, S.; Ochterski, J.; Petersson, G. A.; Ayala, P. Y.; Cui, Q.; Morokuma, K.; Malick, D. K.; Rabuck, A. D.; Raghavachari, K.; Foresman, J. B.; Cioslowski, J.; Ortiz, J. V.; Stefanov, B. B.; Liu, G.; Liashenko, A.; Piskorz, P.; Komaromi, I.; Gomperts, R.; Martin, R. L.; Fox, D. J.; Keith, T.; Al-Laham, M. A.; Peng, C. Y.; Nanayakkara, A.; Gonzalez, C.; Challacombe, M.; Gill, P. M. W.; Johnson, B. G.; Chen, W.; Wong, M. W.; Andres, J. L.; Head-Gordon, M.; Replogle, E. S.; Pople, J. A. *Gaussian 98*, revision A.1; Gaussian, Inc.: Pittsburgh, PA, 1998.

(20) Leach, A. R. *Molecular Modelling Principles and Applications*, 2nd ed.; Prentice Hall: Dorchester, U.K., 2001.

Table 1. Energies of the Most Stable Conformations of Cyclophanes 1−6

		HF/3-21G*			B3LYP/3-21G*		
structure	sym[a]	energy, au	ΔE,[b] kJ/mol	ΔE,[c] kJ/mol	energy, au	ΔE,[b] kJ/mol	ΔE,[c] kJ/mol
1a	C_2	−878.872 653	0	58.6	−884.834 970	0	48.7
1b	C_s	−878.869 602	8.01		−884.832 460	6.59	
2a	C_1	−878.885 681	0	24.4	−884.846 009	0	19.7
2b	C_1	−878.884 005	4.40		−884.844 419	4.18	
2c	C_1	−878.878 603	18.6		−884.840 460	14.6	
3a	C_s	−878.876 920	0	47.4	−884.838 617	0	39.1
3b	C_1	−878.868 220	22.8		−884.831 813	17.9	
3c	C_s	−878.849 394	72.3		−884.816 218	58.8	
4a	C_1	−878.888 158	0	17.9	−884.847 913	0	14.7
4b	C_1	−878.885 148	7.90		−884.845 860	5.39	
4c	C_1	−878.876 359	31.0		−884.838 709	24.2	
5a	C_s	−878.894 965	0	0	−884.853 514	0	0
5b	C_1	−878.893 784	3.10		−884.852 272	3.26	
5c	C_1	−878.885 975	23.6		−884.846 401	18.7	
6a	C_1	−878.894 654	0	0.82	−884.853 177	0	0.89
6b	C_1	−878.892 665	5.22		−884.851 913	3.32	
6c	C_1	−878.892 049	6.84		−884.850 997	5.72	

[a] Symmetries are taken from the HF/3-21G* calculations and are same in the B3LYP/3-21G* calculations. [b] ΔE energies are relative to the energy of the lowest energy conformation. [c] ΔE energies are relative to the energy of the lowest energy cyclophane.

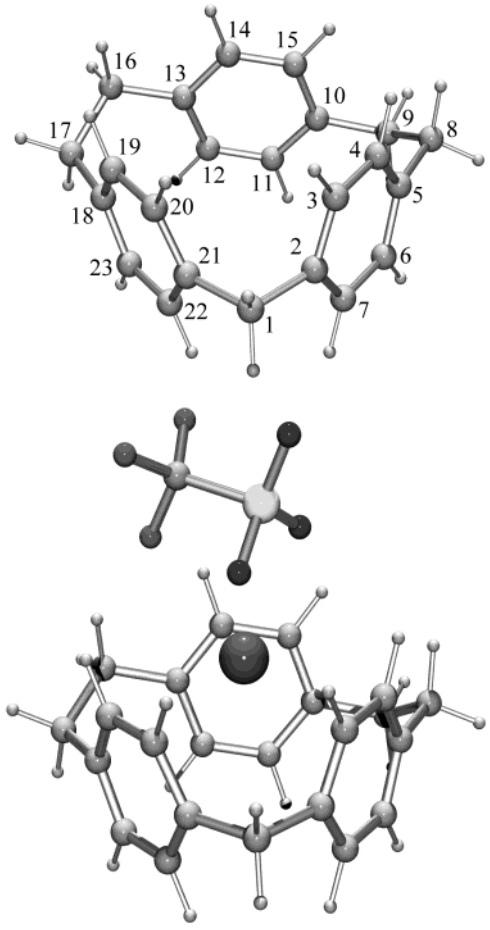

Figure 2. Structures of **1a** and **1ab** calculated at the HF/3-21G* level of theory.

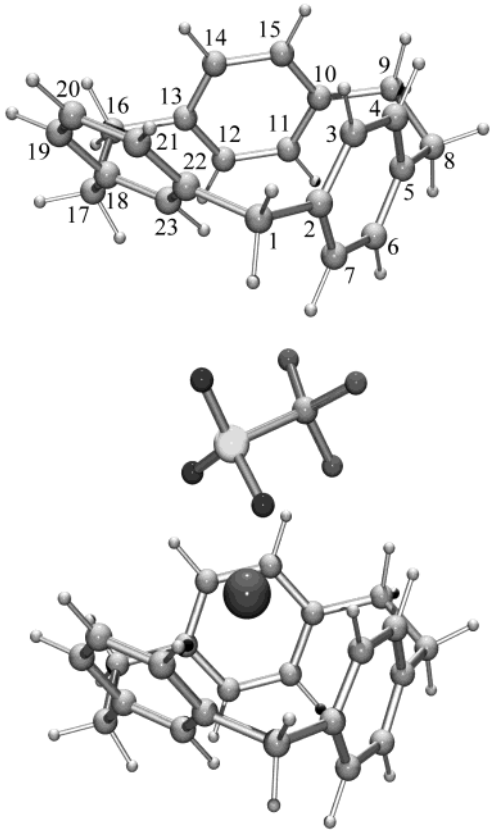

Figure 3. Structures of **2a** and **2aa** calculated at the HF/3-21G* level of theory.

was not visible for the cyclophanes **7**−**10**, and it indicates lower flexibility and fewer available conformations of **1**−**6**. Also the energy difference, 58.6 kJ/mol (HF/3-21G*) and 48.7 kJ/mol (B3LYP/3-21G*), between the lowest energy **5** and the highest energy **1** is larger than in **7**−**10**, 32.7 kJ/mol (HF/3-21G*) and 29.5 kJ/mol (B3LYP/3-21G*). The observed rigidity is due to the change of one flexible ethylene bridge to a more rigid methylene bridge in **1**−**6**. The lowest energy conformations of **1**−**6** calculated at the HF/3-21G* level of theory are shown in Figures 2−7. The synthesized cyclophanes **1** and **3** seem to be the two cyclophanes with highest energy. Optimizations using DFT produce similar results, although given energies are systematically smaller than with the HF method.

The HF/3-21G* calculated bond parameters of **1**−**6** and those taken from available X-ray structures (cyclophanes **1** and **3**) are shown in Table 2. The structural differences resulting in conformations of different point group symmetries (Table 1) are mainly due to changes in torsion angles of the two bridging ethane building

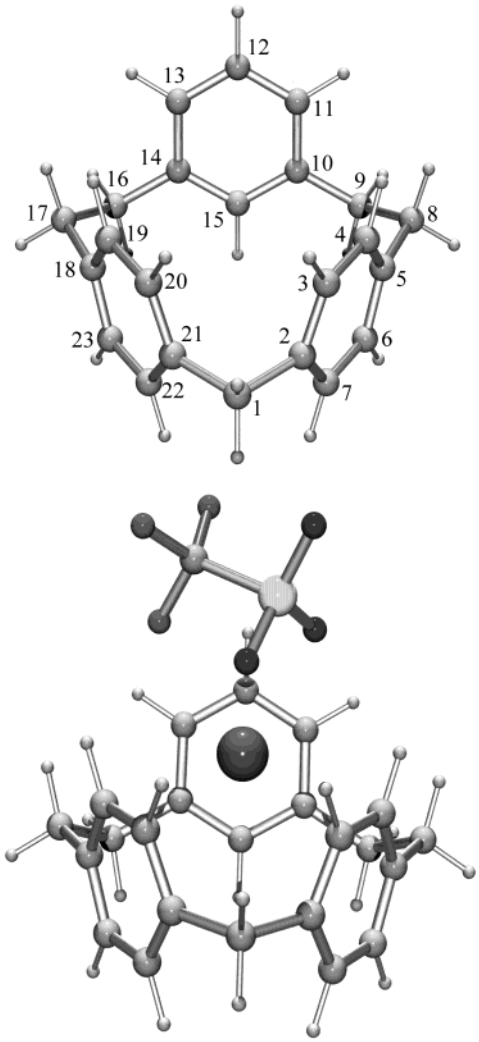

Figure 4. Structures of **3a** and **3aa** calculated at the HF/3-21G* level of theory.

blocks. Though the cyclophanes **1**−**6** are more rigid than **7**−**10**, they still have small energy differences between conformations and are thus capable of adapting to different conformations when complexing metal ions. The calculated lowest energy conformations **1a** and **3a** give geometries similar to those of the corresponding experimental X-ray structures. The overlay pictures of X-ray structures and the HF/3-21G* calculated conformations **1a** and **3a** are shown in Figure 8.

Silver Triflate Complexes. Tables 3 and 4 show the calculated energies of the π-prismand−silver triflate complexes. Calculated and X-ray bond parameters of the complexes are shown in Tables 6 and 7. The complexation of **1**−**6** with silver triflate does not seem to alter conformations of the ligands radically, as seen by comparing the HF calculated bond angles presented in Tables 2, 6, and 7. Some differences in complex structures resulting from optimizations using HF/3-21G* and B3LYP/3-21G* can be observed in Tables 6 and 7. It can be noticed that Ag−C bond lengths produced by B3LYP are generally shorter than corresponding HF-generated bond lengths. The opposite trend is shown in ligand C−C bond lengths, where B3LYP produces slightly longer bonds than HF. For example, in **1ab** the bond length between carbon atoms C1 and C2 is 152.9 pm by HF and 153.1 pm by B3LYP; similarly, for the bond

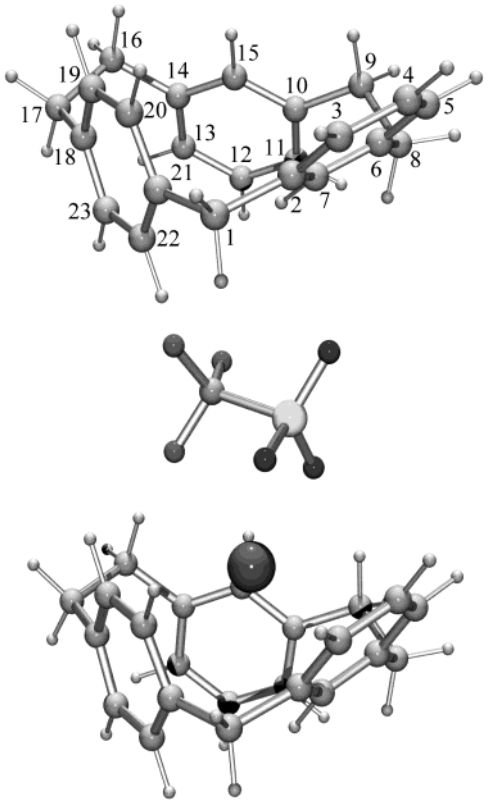

Figure 5. Structures of **4a** and **4aa** calculated at the HF/3-21G* level of theory.

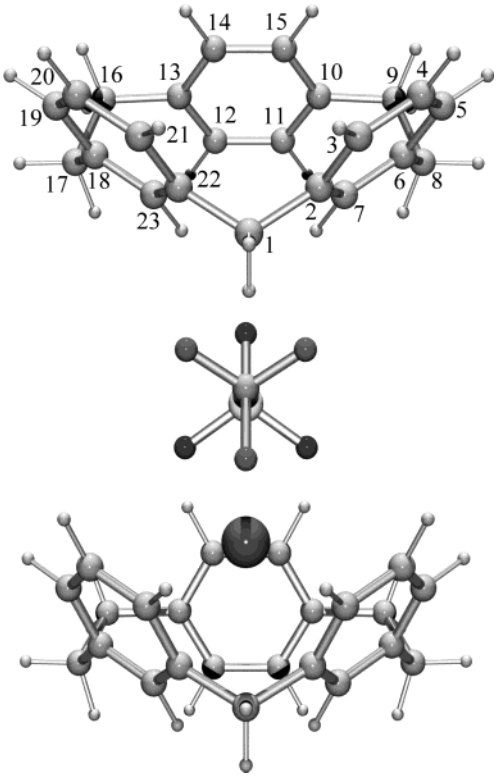

Figure 6. Structures of **5a** and **5aa** calculated at the HF/3-21G* level of theory.

C8−C9 HF gives 156.2 pm and B3LYP 156.6 pm. These two trends combined have some effect on complexed ligand geometries, which is clearly shown by changes in Ag−C bond lengths in general and especially in torsion angles of the meta-bonded phenyl rings. The

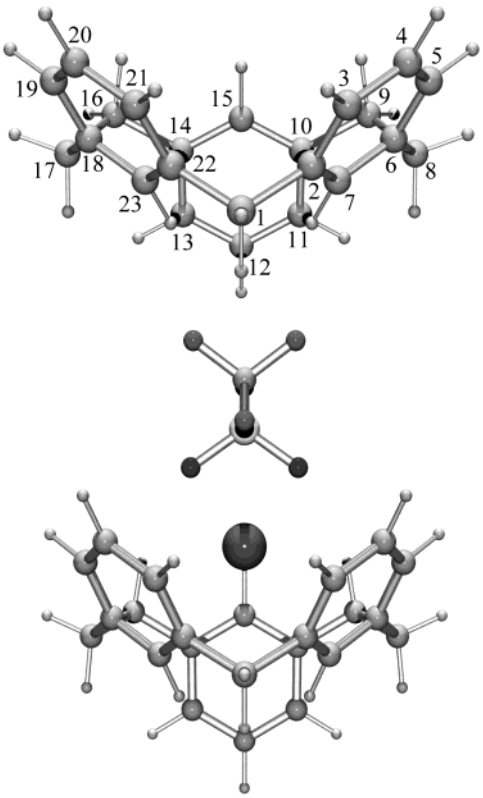

Figure 7. Structures of **6a** and **6aa** calculated at the HF/3-21G* level of theory.

overall bonding trend is still similar regardless of the method used.

Table 3 shows the complex formation energies calculated at the HF/3-21G* level of theory. Complex formation between the lowest energy **5a** and silver triflate creates the lowest energy complex **5aa**. Complexes **6aa** and **1aa** also retain the order of incresing energy, **6aa** being the second lowest in energy and **1aa** being the highest in energy. The complex formation does not retain the order of increasing energy in the other complexes. Optimizations at the B3LYP/3-21G* level of theory, shown in Table 4, estimate that complexes **6aa** and **5aa** change places, **6aa** being the lowest energy complex. The complex **1aa** retains its highest energy position, but **4aa** is now lower in energy than **3ab**, which has become the lowest energy conformation of the **3a**−silver triflate complex.

The HF/3-21G* estimated energy difference between the lowest energy complex **5aa** and the highest energy complex **1aa** is 39.4 kJ/mol, which is more than twice the energy difference (16.6 kJ/mol) between the lowest and the highest Ag^+ complexes of **7**−**10**. For comparison the B3LYP/3-21G* calculated energy difference between the lowest energy complex **6aa** and the highest energy complex **1aa** is 20.1 kJ/mol, which is the same in magnitude as the energy difference (19.6 kJ/mol) between the lowest and the highest energy Ag^+ complexes of **7**−**10** calculated using the same method and basis set.

The energy differences between two conformations of one complex change radically, depending on the shape of the ligand. The energy difference of the conformations **1aa** and **1ab** of the silver triflate complex of the planar ligand **1a** with C_2 symmetry is 0. On the other hand, the energy difference of conformations **6aa** and **6ab** in the complex of the bowl-shaped ligand **6a** is high, 62.7 kJ/mol (HF/3-21G*). This means that, depending on the shape of the ligand, the complex formation is energetically more favored from one direction than from the other.

The effect of the bonding due to complexation can be estimated by calculating the complex formation energy ΔH(cf) for the hypothetical reaction

$$\text{silver triflate} + \pi\text{-prismand} \rightarrow [(\pi\text{-prismand})\text{silver triflate}] \quad (1)$$

using the formula

$$\Delta H(\text{cf}) = E([(\pi\text{-prismand})\text{silver triflate}]) - E(\pi\text{-prismand}) - E(\text{silver triflate}) \quad (2)$$

The energy values of the corresponding cyclophane conformation are used in the formula. The calculated ΔH(cf) values are, however, overestimates of the true value. The discrepancy arises from the phenomenon known as the basis set superposition error (BSSE). The energy of the complexed system falls not only because of the favorable intermolecular interactions but also because the basis set functions on each molecule provide a better description of the electronic structure around the other molecule.[20] Here we have used the counterpoise correction method to estimate the BSSE error, which is calculated by the formula

$$\Delta E(\text{cp-cor}) = E(\pi\text{-prismand})^*[\text{xy}] + E(\text{silver triflate})^*[\text{xy}] - E(\pi\text{-prismand})^*[\text{x}] - E(\text{silver triflate})^*[\text{y}] \quad (3)$$

where the asterisk denotes the complex geometry, [xy] the complex basis set, [x] the π-prismand basis set, and [y] the silver triflate basis set.[21] The idea is to calculate the π-prismand single-point energy at complex geometry in the presence of "ghost" orbitals of the silver triflate and then to subtract the single-point energy of the π-prismand using only its own orbitals at the complex geometry. This way we can calculate the BSSE for the π-prismand part; the same calculation is performed for silver triflate in the presense of π-prismand "ghost" orbitals. The resulting energies added together gives the basis set superposition error. The counterpoise corrected complex formation energy is then calculated by the formula

$$\Delta H(\text{cf,cp-cor}) = \Delta H(\text{cf}) - \Delta E(\text{cp cor}) \quad (4)$$

The complex formation energies calculated at HF/3-21G* and B3LYP/3-21G* levels of theory are shown in Tables 3 and 4. According to the calculated ΔE(cp-cor) values, the BSSE was shown to be unexpectedly large, about three-fourths of the ΔH(cf) values. Details of the counterpoise correction calculations are shown in the Supporting Information. The corrected complex formation energy ΔH(cf,cp-cor) values, except for B3LYP/3-21G* calculated **5ab**, are all negative and thus exothermic, favoring the formation of silver triflate complexes. The three most stable complex conformations calculated with both methods are **1aa**, **1ab**, and **3aa**.

(21) Jensen, F. *Introduction to Computational Chemistry*; Wiley: Chichester, U.K., 1999.

Table 2. Bond Parameters (in pm and deg) of Cyclophanes 1−6 Calculated at the HF/3-21G* Level of Theory Together with the Experimental Values Where Available

atoms	X-ray	**1a**	**1b**	atoms	**2a**	**2b**	**2c**	atoms	X-ray	**3a**	**3b**	**3c**
21−1	152.0	152.7	152.8	22−1	153.4	152.9	153.2	21−1	152.0	152.8	152.9	153.4
1−2	151.9	152.7	152.8	1−2	151.7	152.0	151.8	1−2	152.7	152.8	153.0	153.4
5−8	150.9	151.6	151.8	5−8	151.5	151.6	151.6	5−8	150.9	151.4	151.3	152.3
8−9	155.2	156.2	156.1	8−9	156.6	156.7	157.2	8−9	154.6	155.7	156.1	154.5
9−10	152.0	152.2	152.2	9−10	151.8	152.0	151.6	9−10	151.1	152.3	152.4	153.2
13−16	152.4	152.2	152.2	13−16	151.6	152.0	152.5	14−16	152.0	152.3	153.2	153.2
16−17	154.0	156.2	156.1	16−17	155.6	155.5	154.2	16−17	153.2	155.7	154.7	154.5
17−18	150.9	151.6	151.8	17−18	151.8	151.8	153.0	17−18	150.5	151.4	152.0	152.3
21−1−2	105.0	104.5	104.2	22−1−2	110.5	109.9	112.2	21−1−2	102.5	103.3	102.0	100.5
5−8−9	111.9	112.4	113.5	5−8−9	111.8	112.0	111.9	5−8−9	113.2	111.4	110.5	116.2
8−9−10	113.9	114.8	115.1	8−9−10	113.1	113.7	111.7	8−9−10	115.0	114.9	114.4	118.8
13−16−17	114.4	114.8	115.1	13−16−17	112.8	113.8	116.6	14−16−17	115.3	114.9	118.9	118.8
16−17−18	111.9	112.4	113.5	16−17−18	113.4	113.6	117.6	16−17−18	111.8	111.4	114.5	116.2
20−21−1−2	−84.2	−87.1	−88.0	21−22−1−2	−134.7	−124.7	−140.3	20−21−1−2	−77.4	−81.2	−89.3	−81.2
4−5−8−9	−117.3	−114.1	−50.8	4−5−8−9	−60.4	−111.4	−68.4	4−5−8−9	−125.9	−108.4	−92.7	−15.0
14−13−16−17	−130.2	−128.6	−118.9	14−13−16−17	−98.7	−122.3	−10.9	13−14−16−17	−68.1	−65.3	−169.9	−147.9
5−8−9−10	47.5	45.3	−41.9	5−8−9−10	−40.2	36.5	−36.7	5−8−9−10	62.3	58.8	70.0	−53.5
13−16−17−18	47.5	45.3	41.9	13−16−17−18	65.8	68.9	−65.9	14−16−17−18	−65.2	−58.8	58.6	53.5

atoms	**4a**	**4b**	**4c**	atoms	**5a**	**5b**	**5c**	atoms	**6a**	**6b**	**6c**
21−1	151.6	151.6	151.4	22−1	152.4	152.4	151.7	22−1	152.3	151.7	152.6
1−2	153.2	153.5	153.7	1−2	152.4	152.4	153.4	1−2	152.3	153.3	152.1
6−8	151.9	151.8	152.7	6−8	151.6	151.7	151.8	6−8	151.5	151.5	152.0
8−9	156.2	155.1	154.7	8−9	155.8	155.6	156.0	8−9	155.7	155.4	155.2
9−10	152.3	152.6	152.5	9−10	151.5	151.5	151.3	9−10	152.0	152.0	152.0
14−16	152.0	152.1	152.9	13−16	151.5	151.5	152.0	14−16	152.0	151.9	151.8
16−17	155.8	156.1	155.3	16−17	155.8	155.6	155.3	16−17	155.7	155.6	155.8
17−18	151.2	151.3	152.0	17−18	151.6	151.7	152.5	17−18	151.6	151.6	151.7
21−1−2	109.5	109.3	110.6	22−1−2	111.4	114.5	114.7	22−1−2	109.4	113.2	112.6
6−8−9	113.2	113.9	117.7	6−8−9	112.1	112.3	112.5	6−8−9	112.3	112.3	114.0
8−9−10	114.6	117.1	115.9	8−9−10	111.8	111.7	110.7	8−9−10	113.5	114.1	113.8
14−16−17	113.0	113.1	117.2	13−16−17	111.8	111.7	113.8	14−16−17	113.5	113.1	113.1
16−17−18	110.4	110.5	113.9	16−17−18	112.1	112.3	116.2	16−17−18	112.3	112.6	112.6
20−21−1−2	−73.3	−71.4	−75.0	21−22−1−2	−94.9	131.9	95.9	21−22−1−2	−91	−101.2	−139.5
5−6−8−9	−98.2	−80.4	−167.4	5−6−8−9	−80.4	−77.3	−86.5	5−6−8−9	−97	81.1	130.8
13−14−16−17	72.5	−64.5	−158.0	14−13−16−17	−96.2	−68.0	45.9	13−14−16−17	69.5	64.2	93.6
6−8−9−10	−90.7	−69.2	68.9	6−8−9−10	−60.2	−57.0	−61.3	6−8−9−10	−76.6	55.5	−52.7
14−16−17−18	55.1	−55.3	44.8	13−16−17−18	60.2	−57.0	45.6	14−16−17−18	76.6	69.1	75.7

Conformations **5aa** and **5ab** show large Δ*H*(cf,cp-cor) energy differences between conformations and thus indicate the direction preference in complex formation. The order of decreasing stability of the complexes calculated at the HF/3-21G* level of theory is **3aa** > **1aa** > **5aa** > **2aa** > **6aa** > **4aa**, and the corresponding order at the B3LYP/3-21G* level is **1aa** > **3aa** > **2aa** > **5aa** > **6aa** > **4aa**.

Due to a remarkable BSSE in the formation energies of the [2.2.1]cyclophane π-prismand−silver triflate complexes we were forced to estimated its effect also for formation energies of Ag^+ complexes of [2.2.2]cyclophanes **7**−**10** reported in our earlier paper.[12] These calculations are shown in Table 5. The stability order between conformations of each complex has not been affected by BSSE, but the order of lowest energy complexes has indeed changed. The order of decreasing stability of the complexes has been reversed to **10c**−Ag^+ > **9b**−Ag^+ > **8a**−Ag^+ > **7a**−Ag^+, thus showing the large effect of BSSE in these kinds of complexes. The Δ*H*(cf,cp-cor) values for complexes **1**−**6** are about 150 kJ/mol higher than the values calculated for cyclophanes **7**−**10** and their complexes with Ag^+ ion, thus showing weaker bonding between ligands **1**−**6** and silver triflate. The strength of the three η^2 Ag−C interactions to double bonds on each phenyl moiety of the [2.2.2]cyclophanes **7**−**10** can be compared to three moderately strong hydrogen bonds, each having bond enthalpies of about 60 kJ/mol. This strong interaction can mainly be attributed to the absence of the triflate moiety in these calculations, which will be shown later in this paper.

NBO analyses were carried out for the lowest energy complex conformations at the HF/3-21G* level of theory. Natural charges and Mayer NAO valencies (total atomic bond orders)[22−24] of all non-hydrogen atoms and overlap-corrected bond orders for Ag^+ and for the atoms surrounding it are given in the Supporting Information.

Conformation **1ab** was chosen for NBO analysis, due to its similarity with the X-ray structure and its equal energy with **1aa**. NBO analysis calculated at the HF/3-21G* level of theory reveals that the silver ion has bonded to all three aromatic rings (bond orders ∼0.027). The bond orders from Ag to C3 and C4 in one aromatic ring are almost equal, 0.027 and 0.025, respectively, which is also supported by the similar bond lengths Ag−C3 and Ag−C4 shown in Table 6. Similar bonding is also noticed between Ag and C19 and C20 (bond orders 0.027 and 0.028). Bonding of the silver ion to the third aromatic ring shows different behavior. Bond lengths from Ag to C14 and C15 are different, the Ag−C14 bond being shorter. The NBO analysis shows that Ag^+ is bound not only to C14 and C15 (bond orders 0.033 and 0.021) but also to C13 (bond order 0.015). The strongest interaction and shortest bond length is be-

(22) Mayer, I. *Chem. Phys. Lett.* **1983**, *97*, 270.
(23) Mayer, I. *Theor. Chim. Acta* **1985**, *67*, 315.
(24) Mayer, I. *Int. J. Quantum Chem.* **1986**, *29*, 73.

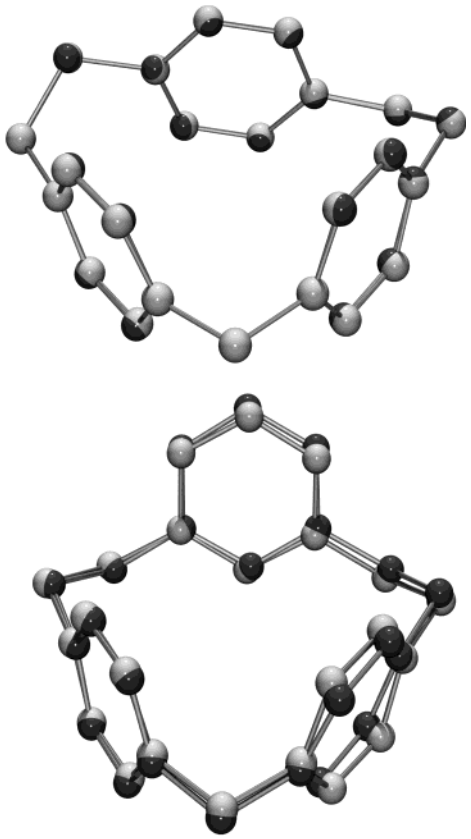

Figure 8. Overlay of HF/3-21G*-optimized (light gray) conformations **1a** (top) and **3a** (bottom) with X-ray structures (dark gray). Hydrogen atoms are omitted for clarity.

Table 3. Energies of the π-Prismand−Silver Triflate and π-Prismand−Ag^+ Complexes Calculated at the HF/3-21G* Level of Theory

complex	energy, au	Δ*E*,[a] kJ/mol	Δ*E*,[b] kJ/mol	Δ*H*(cf),[c] kJ/mol	Δ*E*(cp-cor),[d] kJ/mol	Δ*H*(cf, cp-cor),[e] kJ/mol
1aa	−7 006.171 302	0	39.4	−202.3	−153.5	−48.7
1ab	−7 006.171 301	0.00	39.4	−202.3	−153.5	−48.7
2aa	−7 006.177 330	0	23.6	−183.9	−145.1	−38.8
2ab	−7 006.169 159	21.5	45.0	−162.4	−142.2	−20.2
3aa	−7 006.174 225	0	31.7	−198.7	−147.7	−51.1
3ab	−7 006.169 911	11.3	43.0	−187.4	−161.2	−26.2
4aa	−7 006.174 024	0	32.2	−168.7	−144.0	−24.7
4ab	−7 006.166 174	20.6	52.8	−148.1	−138.6	−9.50
5aa	−7 006.186 300	0	0	−183.1	−134.7	−48.4
5ab	−7 006.163 607	59.6	59.6	−123.5	−121.2	−2.28
6aa	−7 006.183 752	0	6.69	−177.2	−139.6	−37.6
6ab	−7 006.159 885	62.7	69.4	−114.5	−106.5	−7.99
1ab−Ag^+ [f]	−6 052.588 613			−303.0	−121.6	−181.4
3aa−Ag^+ [f]	−6 052.594 212			−306.5	−120.0	−186.5
silver triflate	−6 127.221 615					
Ag^+	−5 173.600 559					

[a] Δ*E* energies are relative to the energy of the lowest energy conformation. [b] Δ*E* energies are relative to the energy of the lowest energy complex. [c] Equation 2. [d] Equation 3. [e] Equation 4. [f] For complexes **1ab**−Ag^+ and **3aa**−Ag^+ eqs 2 and 3 contain energy terms for Ag^+ in place of silver triflate.

tween Ag and carbon atom C14. Optimization of **1ab** at the B3LYP/3-21G* level of theory shows a similar trend in bonding, which can be seen by the similar bond lengths and angles in Table 6.

In the X-ray structure of **1**−silver triflate the silver ion is bound deeper into the cavity of the ligand than in the calculated **1ab**. This can be seen in Figure 9 and from the bond angles in Table 6. HF/3-21G* single-point

Table 4. Energies of the π-Prismand−Silver Triflate Complexes Calculated at the B3LYP/3-21G* Level of Theory

complex	energy, au	Δ*E*,[a] kJ/mol	Δ*E*,[b] kJ/mol	Δ*H*(cf),[c] kJ/mol	Δ*E*-(cp-cor),[d] kJ/mol	Δ*H*(cf, cp-cor),[e] kJ/mol
1aa	−7 017.802 344	0	20.1	−260.8	−205.9	−54.9
1ab	−7 017.802 344	0	20.1	−260.8	−205.9	−54.9
2aa	−7 017.804 848	0	13.5	−238.4	−198.0	−40.4
2ab	−7 017.799 736	13.4	26.9	−225.0	−191.2	−33.8
3aa	−7 017.800 688	4.60	24.4	−246.9	−203.1	−43.8
3ab	−7 017.802 442	0	19.8	−251.5	−210.2	−41.3
4aa	−7 017.803 475	0	17.1	−229.8	−203.7	−26.1
4ab	−7 017.797 055	16.9	34.0	−212.9	−195.2	−17.7
5aa	−7 017.808 769	0	3.22	−229.0	−195.4	−33.5
5ab	−7 017.794 075	38.6	41.8	−190.4	−203.0	12.5
6aa	−7 017.809 997	0	0	−233.1	−202.8	−30.3
6ab	−7 017.786 478	61.8	61.8	−171.4	−156.5	−14.9
silver triflate	−6 132.868 036					

[a] Δ*E* energies are relative to the energy of the lowest energy conformation. [b] Δ*E* energies are relative to the energy of the lowest energy complex. [c] Equation 2. [d] Equation 3. [e] Equation 4.

calculation and NBO analysis of the X-ray structure of **1**−silver triflate was carried out in order to compare the bond orders of **1ab** and the X-ray structure. The bonding trend observed is similar to the calculated complex conformation. The silver ion forms bonds to the same atoms in the ligand as in **1ab**. In the X-ray structure the silver atom is bonded to carbon atoms C3 and C4 with bond orders of 0.026 and 0.027, to carbons C13, C14, and C15 with bond orders of 0.010, 0.033, and 0.030, and to carbon atoms C19 and C20 with bond orders of 0.023 and 0.041. The bond orders of **1ab** and those of the X-ray structure of **1**−silver triflate seem to be almost similar in magnitude, although bond orders to carbons C15 and C20 are higher in the X-ray structure than in **1ab**, as indicated by shorter bond lengths.

To estimate the effect of the triflate moiety on the position of the silver ion in the cavity of the ligand in the calculated complexes, an optimization of a complex of **1ab** without the triflate moiety, **1ab**−Ag^+, was performed. As can be seen from Table 6, the bond angles indicate that the silver ion is deeper in the cavity of the ligand than in **1ab** and in the X-ray structure of **1**−silver triflate. The NBO analysis was also calculated for **1ab**−Ag^+. It shows that bond orders between the silver ion and carbon atoms in the aromatic rings are generally higher than in **1ab** and in the X-ray structure of **1**−silver triflate. In the structure **1ab**−Ag^+ the silver ion is bound to carbon atoms C3 and C4 with bond orders of 0.034 and 0.033, respectively. In addition to this, the bond orders between Ag^+ and carbon atoms C2 and C5 have become significant, being 0.012 and 0.014. This is also observed in other phenyl rings. The bond orders between the silver ion and carbon atoms C13, C14, and C15 are 0.021, 0.037, and 0.030, respectively. Bond orders between Ag^+ and carbon atoms C10 and C12 have also become significant: 0.013 and 0.010, respectively. The bond orders between Ag^+ and C19 and C20 are 0.033 and 0.036, and bond orders to C18 and C21 are now both 0.012. This enhanced bonding can also be seen in complex formation energies calculated at the HF/3-21G* level of theory for **1ab**−Ag^+ and **3aa**−Ag^+ in Table 3. In both cases the silver atom ion is shown to form 130 kJ/mol stronger interactions with ligand when compared to complexes where the triflate moiety is present as a counterpart. Complex formation energies

Table 5. Energies of the [2.2.2]Cyclophanes 7−10 and Their π-Prismand−Ag^+ Complexes Calculated at the HF/3-21G* Level of Theory

π-prismand	energy, au	complex	energy, au	Δ*E*,[a] kJ/mol	Δ*E*,[b] kJ/mol	Δ*H*(cf),[c] kJ/mol	Δ*E*(cp-cor),[d] kJ/mol	Δ*H*(cf,cp-cor),[e] kJ/mol
7a	−917.700 344	**7a**−Ag^+	−6 091.425 621	0	16.6	−327.7	−127.6	−199.9
7b	−917.699 108	**7b**−Ag^+	−6 091.423 344	5.98		−321.7	−130.7	−194.0
8a	−917.707 539	**8a**−Ag^+	−6 091.430 298	0	4.31	−321.1	−120.6	−200.2
8c	−917.701 295	**8c**−Ag^+	−6 091.422 370	20.8		−300.2	−120.5	−195.9
8b	−917.705 701	**8b**−Ag^+	−6 091.422 313	21.0		−300.1	−119.8	−184.9
9b	−917.710 328	**9b**−Ag^+	−6 091.431 939	0	0	−315.5	−116.9	−201.0
9a	−917.711 303	**9a**−Ag^+	−6 091.427 501	11.7		−303.8	−132.5	−171.1
9d	−917.705 371	**9d**−Ag^+	−6 091.415 861	42.2		−273.2	−130.6	−158.0
9c	−917.707 665	**9c**−Ag^+	−6 091.410 708	55.8		−259.7	−125.0	−144.1
10c	−917.703 234	**10c**−Ag^+	−6 091.427 876	0	10.7	−300.9	−111.5	−214.3
10d	−917.707 613	**10d**−Ag^+	−6 091.427 826	0.13		−300.8	−112.0	−202.2
10a	−917.712 238	**10a**−Ag^+	−6 091.424 358	9.25		−291.7	−117.3	−175.6
10b	−917.712 780	**10b**−Ag^+	−6 091.411 994	41.7		−259.2	−112.1	−147.0
Ag^+	−5 173.600 559							

[a] Δ*E* energies are relative to the energy of the lowest energy conformation. [b] Δ*E* energies are relative to the energy of the lowest energy complex. [c] Δ*H*(cf) = *E*([(π-prismand)Ag^+]) − *E*(Ag^+) − *E*(π-prismand)). [d] Δ*E*(cp-cor) = *E*(π-prismand)*[xy] + *E*(Ag^+)*[xy] − *E*(π-prismand)*[x] − *E*(Ag^+)*[y], where the asterisk denotes complex geometry, [xy] the complex basis set, [x] the π-prismand basis set, and [y] the silver triflate basis set. [e] Equation 4.

Table 6. Bond Parameters (in pm and deg) of HF/3-21G*- and B3LYP/3-21G*-Optimized and X-ray Structures of π-Prismand−Silver Triflate and π-Prismand−Ag^+ Complexes

	HF		B3LYP			HF		B3LYP	
1−silver triflate	1ab	**1ab**−Ag^+	1ab	X-ray	**3**−silver triflate	3aa	**3aa**−Ag^+	3aa	X-ray
Ag−C3	272.6	267.9	262.6	252.0	Ag−C3	284.9	273.4	268.6	265.9
Ag−C4	276.7	272.0	270.8	257.7	Ag−C4	278.4	268.4	274.3	256.7
Ag−C14	262.8	263.7	250.5	243.9	Ag−Ct (C10−C15)	271.5	261.7	267.3	261.0
Ag−C15	284.8	275.8	275.8	252.3	Ag−C15	303.7	267.4	330.0	255.1
Ag−C19	279.4	276.0	268.9	266.1	Ag−C19	274.3	268.6	265.2	262.1
Ag−C20	273.8	268.3	262.9	245.2	Ag−C20	283.5	273.4	265.0	268.3
Ag−O1	261.3		258.7	253.1	Ag−O1	272.1		268.0	236.6
Ag−O2	255.6		252.5	301.6	Ag−O2	250.6		250.1	371.5
Ag−F1	279.0		274.5	432.2	Ag−F1	272.8		264.4	398.9
C6−C4−Ag	99.1	84.3	102.5	96.8	C6−C4−Ag	102.4	86.5	105.7	94.9
C12−C14−Ag	90.3	78.0	94.2	96.3	C15−C12−Ag	63.0	52.5	74.2	49.1
C22−C20−Ag	98.2	84.9	98.9	100.3	C22−C20−Ag	100.3	86.5	103.5	92.8
C2−C5−Ag	63.5	60.6	62.1	62.2	C2−C5−Ag	67.9	64.2	63.9	65.6
C10−C13−Ag	70.9	65.0	71.5	67.9	C10−C14−Ag	67.3	64.4	68.5	62.3
C18−C21−Ag	66.9	65.2	66.3	71.8	C18−C21−Ag	62.9	61.4	65.3	62.2
C20−C21−C1−C2	−87.4	−87.1	−85.2	−79.9	C20−C21−C1−C2	−86.1	−86.4	−85.3	−82.0
C4−C5−C8−C9	−122.7	−123.5	−117.3	−116.1	C4−C5−C8−C9	−113.8	−115.5	−108.2	−106.6
C14−C13−C16−C17	−140.1	−136.4	−135.2	−131.2	C13−C14−C16−C17	−67.7	−65.7	−55.5	−74.9
C21−C1−C2	104.6	104.6	104.4	114.7	C21−C1−C2	103.2	103.3	103.3	102.7
C5−C8−C9−C10	47.7	46.7	47.3	46.2	C5−C8−C9−C10	61.0	59.8	56.0	59.7
C13−C16−C17−C18	46.3	44.5	46.2	46.6	C14−C16−C17−C18	−60.4	−59.7	−55.5	−59.2

of **1ab**−Ag^+ and **3aa**−Ag^+ seem to be about 20 kJ/mol less exothermic than the corresponding formation energies of the strongest [2.2.2]cyclophane π-prismand complexes shown in Table 5.

The triflate moiety in the calculated **1ab** complex prevents the silver ion from moving deeper into the cavity of the π-prismand ligand. To study the enhanced bonding of the triflate moiety toward the silver ion in the calculated complexes, a comparison of geometries of silver triflate moieties was carried out. Figure 10 shows the silver triflate moieties taken from the X-ray structure of **3**−silver triflate and from the optimized structures of **3aa** and free silver triflate. The silver ion in the X-ray structure is bonded mainly to one oxygen atom O1 in the triflate part with a bond order of 0.094 and more weakly to the second oxygen O2 with a bond order of 0.022. In the HF/3-21G* calculated complex **3aa** the silver ion is bound more strongly to the triflate moiety by forming bonds with oxygen atoms O1 and O2 and with fluorine F1 with bond orders of 0.065, 0.083, and 0.043, respectively. The effect of the π-prismand ligand on bonding between Ag^+ and the triflate moiety can be seen by comparing the bond lengths observed in **3aa** to bond lengths in optimized free silver triflate. The bonding of silver in the free silver triflate is stronger, which is shown in Figure 10 by shorter bond lengths between silver ion and O1, O2, and F1 than in **3aa**. Both the HF and B3LYP methods produced the same kinds of results. Similar trends are also observed with structures of **1**−silver triflate and can be seen in Table 6 and Figure 9.

The triflate moiety and the π-prismand ligand form a competing pair over the silver ion. In the calculated structures the chemical environment of a complex is absent and generally a complex under study is shown to wrap up into itself more than in the corresponding X-ray structure, where the chemical environment distributes some acting forces over the crystal. Although the triflate moiety in the calculated structures is forming a stronger interaction with silver ion than in the X-ray structures, the π-prismand ligand is still able to participate in complex formation. Generally longer

Table 7. Bond Parameters (in pm and deg) of HF/3-21G*- and B3LYP/3-21G*-Optimized π-Prismand−Silver Triflate Complexes

2−silver triflate	**2aa** HF	**2aa** B3LYP	**4**−silver triflate	**4aa** HF	**4aa** B3LYP	**5**−silver triflate	**5aa** HF	**5aa** B3LYP	**6**−silver triflate	**6aa** HF	**6aa** B3LYP
Ag−C3	267.7	254.8	Ag−C7	271.4	254.0	Ag−C2	284.0	272.8	Ag−C2	280.9	274.5
Ag−C4	301.0	294.8	Ag−Ct (C2−C7)	279.9	282.8	Ag−C3	292.5	331.8	Ag−C7	285.5	256.7
Ag−C14	268.1	254.6	Ag−C10	329.2	306.4	Ag−C14	284.7	293.6	Ag−C10 and Ag−C14	361.0	318.8
Ag−C15	275.4	268.6	Ag−C15	280.4	261.6	Ag−C15	284.7	256.4	Ag−C15	296.7	261.4
Ag−C22	283.1	273.3	Ag−C19	287.1	276.3	Ag−C21	292.5	266.7	Ag−C22	281.0	274.5
Ag−C23	284.0	262.1	Ag−C20	265.9	253.2	Ag−C22	284.0	274.9	Ag−C23	285.5	256.7
Ag−O1	249.6	243.2	Ag−O1	250.6	249.1	Ag−O1	256.1	257.5	Ag−O1	255.3	253.6
Ag−O2	257.6	263.2	Ag−O2	252.1	250.1	Ag−O2	256.1	248.5	Ag−O2	255.3	253.6
Ag−F1	295.7	274.2	Ag−F1	289.5	278.6	Ag−F1	270.8	261.5	Ag−F1	262.2	255.3
C6−C4−Ag	96.7	94.3	C7−C4−Ag	49.7	43.7	C7−C4−Ag	61.8	44.3	C7−C4−Ag	54.0	44.4
C12−C14−Ag	98.6	100.6	C12−C15−Ag	125.8	118.4	C12−C14−Ag	109.7	101.4	C12−C15−Ag	126.2	114.4
C23−C20−Ag	52.7	44.7	C22−C20−Ag	94.1	92.2	C23−C20−Ag	61.8	66.6	C23−C20−Ag	54.0	47.4
C2−C5−Ag	55.0	52.2	C2−C6−Ag	64.2	63.5	C2−C6−Ag	54.1	59.6	C2−C6−Ag	58.4	59.4
C10−C13−Ag	67.4	68.9	C10−C14−Ag	62.7	60.7	C10−C13−Ag	67.2	54.4	C10−C14−Ag	70.4	67.4
C18−C22−Ag	74.2	74.4	C18−C21−Ag	71.9	70.9	C18−C22−Ag	82.2	90.0	C18−C22−Ag	74.1	70.3
C21−C22−C1−C2	−124.4	−134.8	C20−C21−C1−C2	−72.5	−67.5	C21−C22−C1−C2	−89.5	−75.6	C21−C22−C1−C2	−86.9	−89.5
C4−C5−C8−C9	−63.2	−60.7	C5−C6−C8−C9	−90.9	−95.2	C5−C6−C8−C9	−78.5	−97.1	C5−C6−C8−C9	−99.1	−102.1
C14−C13−C16−C17	−115.3	−112.2	C13−C14−C16−C17	59.3	57.3	C14−C13−C16−C17	−112.7	−103.7	C13−C14−C16−C17	60.0	56.3
C22−C1−C2	109.3	110.2	C21−C1−C2	108.3	109.0	C22−C1−C2	109.8	110.9	C22−C1−C2	108.6	109.2
C5−C8−C9−C10	−41.7	−40.4	C6−C8−C9−C10	−80.1	−77.7	C6−C8−C9−C10	−58.2	−67.0	C6−C8−C9−C10	−71.2	−70.2
C13−C16−C17−C18	62.5	65.7	C14−C16−C17−C18	50.3	76.9	C13−C16−C17−C18	58.2	49.3	C14−C16−C17−C18	71.2	70.2

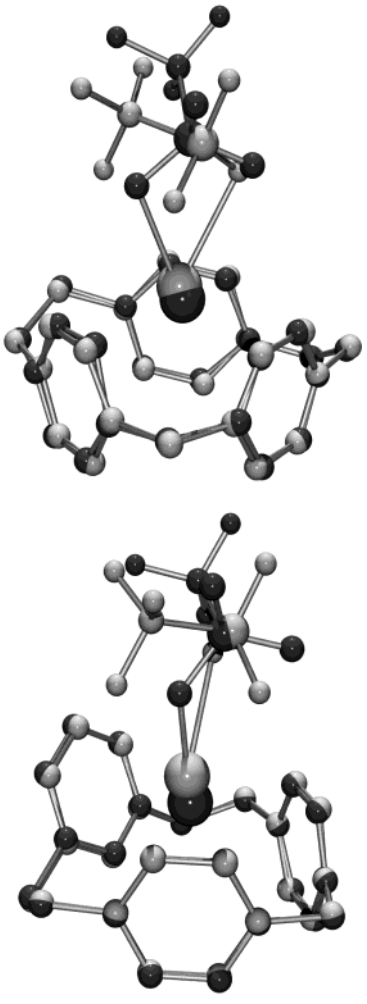

Figure 9. Overlay of HF/3-21G*-optimized (light gray) conformations **1ab** (top) and **3aa** (bottom) with X-ray structures (dark gray). Hydrogen atoms are omitted for clarity.

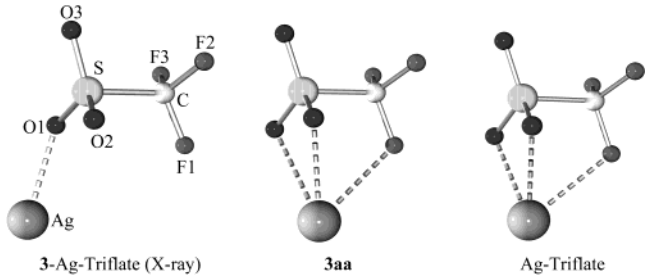

Figure 10. Structures of silver triflate moieties taken from the X-ray structure of **3**−silver triflate and HF/3-21G*-optimized structures of **3aa** and free silver triflate structure. Selected bond distances (pm) are as follows. **3**−silver triflate: Ag−O1, 236.6; Ag−O2, 371.5; Ag−F1, 398.9. HF/3-21G*-optimized distances (pm) are as follows. **3aa**: Ag−O1, 272.1; Ag−O2, 250.6; Ag−F1, 272.8. Silver triflate: Ag−O1, 242.3; Ag−O2, 42.3; Ag−F1, 262.2. B3LYP/3-21G*-optimized distances (pm) are as follows. **3aa**: Ag−O1, 268.0; Ag−O2, 250.1; Ag−F1, 264.4. Silver triflate: Ag−O1, 236.4; Ag−O2, 236.4; Ag−F1, 251.5.

Ag−C bond lengths in the calculated π-prismand−Ag complexes as compared to those in the X-ray structures are mainly due to different bonding of the triflate moiety but are also due to the chosen basis set and the method of calculation.

The NBO analysis shows that in **2aa** the silver ion is bound to the carbon atoms C3 and C4 of the para-bonded phenyl ring with bond orders of 0.030 and 0.015. The Ag−C3 bond is much shorter than the Ag−C4 bond, which can be seen in Table 7. The silver atom is also bound to the carbon atoms C14 and C15 in the second para-bonded phenyl ring with bond orders of 0.031 and 0.026, the Ag−C14 bond being shorter. Almost equal bond orders are found for the bonds Ag−C22 and Ag−C23 in the meta-bonded phenyl ring, 0.020 and 0.024, respectively. A weaker interaction (bond order 0.010) is also found between Ag and C18. In the B3LYP-optimized complex structure of **2aa** the silver atom has moved closer to carbon atom C2, making more shared interactions with carbon atoms C2, C3, and C4. The silver atom also makes a stronger interaction toward carbon atom C23 by the turning of the meta-bonded phenyl ring.

The silver ion in **3aa** is mainly bound to the four carbon atoms C3, C4, C19, and C20 in the two para-bonded phenyl rings, with bond orders of 0.023, 0.028, 0.032, and 0.024, respectively. The same trend is also evident in the X-ray structure of **3**−silver triflate (Table 4 and Figure 9). A single-point calculation and NBO analysis of the X-ray structure was carried out. In the X-ray structure the silver ion is bound to the carbon atoms C3, C4, C19, and C20 with bond orders of 0.028, 0.035, 0.028, and 0.025. A weak interaction is also noticed between Ag^+ and C5 (bond order 0.010). In **3aa** the silver ion forms an interesting interaction with all carbon atoms (C10−C15) in the meta-bonded phenyl ring with bond orders varying from 0.011 of C12 to 0.017 of C14 and C15. In the X-ray structure the silver ion is deeper in the cavity of the ligand and closer to the carbon atom C15 than the center of the meta-bonded phenyl ring, and so the same kind of interaction as in the calculated model does not occur. The calculated bond orders of the X-ray structure between Ag^+ and C10, C14, and C15 are 0.024, 0.018, and 0.034. The different position of the silver ion can be explained by the absence of the chemical environment in the calculated model and thus by stronger interaction of the triflate moiety over the silver ion as discussed earlier. In the meta-bonded phenyl ring of the B3LYP-optimized **3aa** the silver atom is closer to carbon atoms C11, C12, and C13 than the carbon atom C15.

As mentioned above, an optimization of a complex of **3aa** without the triflate moiety, **3aa**−Ag^+, was also performed. As shown by the bond angles in Table 6, the silver ion in **3aa**−Ag^+ is deeper in the cavity of the ligand than in **3aa** or in the X-ray structure of **3**−silver triflate. The NBO analysis of **3aa**−Ag^+ shows generally higher bond orders and a wider range of bonding carbon atoms but a bonding trend similar to that observed in **3aa** and in the X-ray structure of **3**−silver triflate. The silver ion interacts with the carbon atoms C2, C3, C4, and C5 in one para-bonded ring (bond orders 0.010, 0.033, 0.037, and 0.015) and with the carbon atoms C18, C19, C20, and C21 in the other para-bonded phenyl ring (bond orders 0.015, 0.037, 0.033, and 0.010). In **3aa**−Ag^+ the silver ion interacts with all the carbon atoms in the meta-bonded phenyl ring (bond orders 0.014−0.034) but is mainly emphasized on the carbon atoms C10, C14, and C15.

Conformation **4aa** shows three different interactions between the silver atom and the phenyl rings. On the basis of the NBO analysis the Ag ion is bonded mainly to the carbon C7 (bond order 0.029) in one meta-bonded phenyl ring but also to the adjacent carbon atoms C2 and C6 (bond orders 0.015 and 0.016). Table 7 shows also the distance from Ag^+ to the center of this meta-bonded phenyl ring, which is almost equal to the short distance from Ag^+ to carbon atom C7. Carbons C3, C4, and C5 have only a very small influence on the bonding. Silver ion interacts only with one carbon atom, C15, in the other meta-bonded phenyl ring with a bond order of 0.034. In the para-bonded phenyl ring the two carbon atoms C19 and C20 interact with the silver ion by bond orders of 0.022 and 0.033. As can be seen from Table 7, the Ag−C20 bond is shorter than the Ag−C19 bond. A similar bonding trend was also found by B3LYP/3-21G* optimization.

In **5aa** the silver ion is bound symmetrically to the ligand. It forms similar bonds to both meta-bonded phenyl rings by interacting with carbon atoms C2, C3, and C7 (bond orders 0.021, 0.020, and 0.011) in one phenyl ring and with carbon atoms C21, C22, and C23 (bond orders 0.020, 0.021, and 0.011) in the other. Bonding to the para-bonded phenyl ring is divided equally between carbon atoms C14 and C15 with bond orders of 0.026. Equal bond lengths in Table 7 also show this symmetrical bonding of the silver atom. In the B3LYP-optimized structure the symmetry is lost and both meta-bonded phenyl rings have turned so that the silver atom forms stronger interactions with carbon atoms C2, C7, C21, and C22. Symmetrical interactions with carbon atoms C14 and C15 of the HF-optimized structure have also changed to a closer interaction with C15.

The silver ion in **6aa** is bound to two phenyl rings in a way similar to that in **5aa**. In this structure the Ag^+ is closer to the two phenyl rings which are in a cis conformation and the bonding interaction is divided between more atoms than in the case of **5aa**. The silver ion interacts with carbon atoms C2, C3, C6, and C7 (bond orders 0.020, 0.013, 0.010, 0.023) in one phenyl ring and with carbon atoms C18, C21, C22, and C23 (bond orders 0.010, 0.013, 0.020, and 0.023) in the other phenyl ring. However, Ag^+ bonds only to carbon atom C15 in the third phenyl ring with a bond order of 0.025. In the symmetrical B3LYP-optimized structure of **6aa** the silver atom retains one bond to C15 but has more focused bonding toward carbon atoms C2, C7, C22, and C23 of the two meta-bonded phenyl rings.

Figure 11 summarizes the bonding behavior of the HF/3-21G-optimized π-prismand−silver triflate complexes based on bond orders taken from NBO analysis. As can be seen, the silver ion forms a different set of bonds in every complex. Interactions of the silver ion with a single phenyl ring vary from a η^1 interaction to a η^6 interaction. Electron density in this kind of aromatic ligand is delocalized, and the possibility for bonding and back-bonding interactions of different magnitudes with the metal ion inside the cavity seems to be available regardless of the ligand conformation. The mechanism of the π-bonding between the aromatic ring and the silver ion in the case of bis(*m*-xylene)silver perchlorate has been discussed by Taylor et al.[25] In the case of electron donation from the aromatic to the metal acceptor orbitals, the best position for the metal ion would be in the π-cloud above one of the carbon atoms of the ring, at the position of the highest π-electron density. In the case of electron back-donation from the metal to the aromatic moiety, the best overlap between the filled metal d orbitals and the antibonding π MO's of the aromatic moiety is achieved with the metal in the π cloud equidistant between two carbon atoms of the ring.[25] Both cases are visible in the present complexes, and it can be seen that the shape of the ligand and its conformation plays an important role when the nature of the interaction is established.

Figure 11 shows six complexes and their bonding modes. Comparing the bonding modes, bond orders, and complex formation energies leads to a conclusion. In the

(25) Taylor, I. F., Jr.; Hall, E. A.; Amma, E. L. *J. Am. Chem. Soc.* **1969**, *91*, 5745.

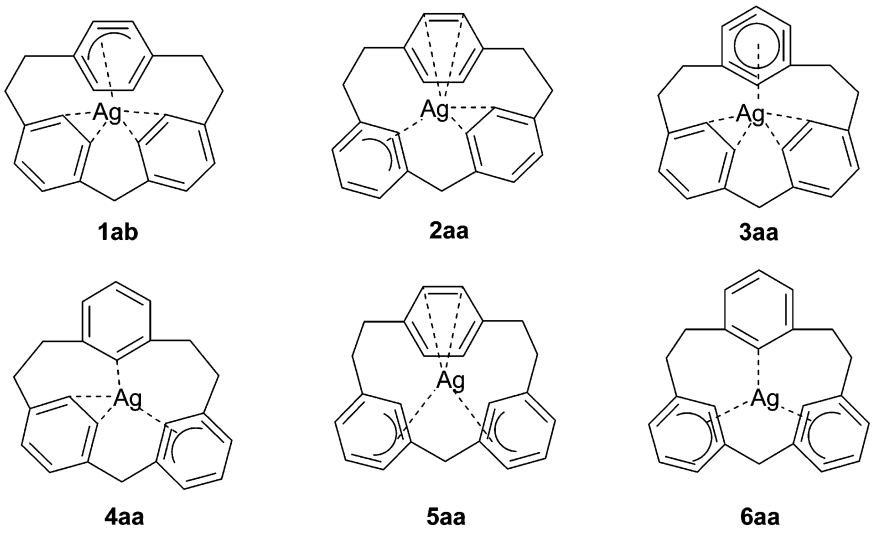

Figure 11. Bonding interactions between the Ag atom and the ligand in π-prismand−silver triflate complexes based on NBO analyses carried out at the HF/3-21G* level of theory. Triflate moieties are omitted for clarity.

Table 8. Natural Charges Obtained from NBO Analyses of π-Prismand−Silver Triflate Complexes at the HF/3-21G* Level of Theory

atom/group	**1ab**	**2aa**	**3aa**	**4aa**	**5aa**	**6aa**	silver triflate
Ag	0.87	0.86	0.86	0.86	0.86	0.85	0.91
triflate	−0.89	−0.89	−0.89	−0.88	−0.89	−0.88	−0.91
silver triflate	−0.02	−0.03	−0.03	−0.02	−0.04	−0.03	0.00
ligand	0.02	0.03	0.03	0.02	0.04	0.03	-

most stable complexes **1ab** and **3aa** the silver ion bonds to two "double bonds", thus supporting a back-bonding component in addition to a σ-bonding component. In these complexes the silver ion is almost symmetrically bound between two carbon atoms of the two phenyl rings. This can been seen in bond orders and bond lengths. Asymmetry of the bonding between two carbon atoms and thus a σ-bonding component increases as we move toward less stable complexes. In **6aa** and **4aa** the bonding of Ag^+ is more diverse and varies between a bond to one carbon atom and a more delocalized interaction to four carbon atoms in one phenyl ring. According to the present results and to previous studies,[11,25,26] it seems that the back-bonding component of the overall bonding is weaker than the σ-bonding component and appears only when the ligand is flexible enough and capable of adapting to the most suitable orientation for complexation.

Table 8 summarizes the natural charges of the silver triflates and ligands of the calculated complexes and free silver triflate calculated at the HF/3-21G* level of theory. The natural charges have been calculated by adding together natural charges of all atoms in a current moiety. As seen in Table 8, all the ligands possess a positive total charge, and silver triflate moieties have a negative charge. Both cyclophane and silver triflate are neutral in the uncomplexed state, and thus complexation produces a charge flow from cyclophane to silver triflate. When the charges of the Ag ions in the complexes are compared to the charge of Ag^+ in a free silver triflate, a similar observation can be made. The positive charge of the Ag ion in a free silver triflate has become less positive after complex formation, thus supporting ligand to metal charge flow in π-prismand−silver triflate complexes. These observations of charge flow indicate that the ligand-to-metal σ-donation is more important than the metal-to-ligand back-bonding component. The same kind of trend was observed for Ag^+ complexes of cyclophanes **7**−**10** reported in our previous paper.[12]

Ag ion is shown to form weak bonds by getting electron density from the hydrocarbon skeleton to the empty 5s orbital and partially donating electron pairs from its valence 4d orbitals to the antibonding π-MO's of the three aromatic rings of the π-prismands. This model of π-complexation was first proposed by Dewar[27] and applied by Chatt and Duncanson[28] in 1953. The strength of the bond can be compared to a hydrogen bond. Hydrogen bonds are usually weak, typically 20−25 kJ/mol, but moderately strong hydrogen bonds can easily have bond enthalpies of 50 kJ/mol and thus are of the same order as silver triflate bonding to the present π-prismands (∼25−50 kJ/mol).[16]

Conclusions

The cyclophanes **1**−**6** form a series of structurally isomeric compounds. They each have the same $C_{23}H_{22}$ skeleton, but the ring size is changed from the 17-membered ring of **1** to the 14-membered ring of **6**. In comparison to [2.2.2]cyclophane π-prismands **7**−**10**, cyclophanes **1**−**6** possess a more strained structure and are capable of fewer possible conformations. Although **1**−**6** have increased rigidity, they still have small energy differences between conformations and thus are capable of adapting to different conformations when complexed with metal ions.

The complexation of cyclophanes **1**−**6** with silver triflate does not seem to alter the conformations of the ligands radically. Complex formation energies, ΔH(cf,cp-cor), for all cyclophanes **1**−**6** were shown to be negative, thus favoring formation of the silver triflate complexes of all [2.2.1]cyclophane π-prismands. The

(26) Hall Griffith, E. A.; Amma, E. L. *J. Am. Chem. Soc.* **1974**, *96*, 743−749.

(27) Dewar, M. J. S. *Bull. Soc. Chim. Fr.* **1951**, *18*, C79.
(28) Chatt, J.; Duncanson, L. A. *J. Chem. Soc.* **1953**, 2939.

complex formation in these cyclophanes shows a direction preference. It is shown that the silver ion is most likely bonded to a more open part of the cyclophane cavity than to a narrower part from the opposing direction.

The rigidity and smaller cavity size of the present cyclophanes compared to [2.2.2]cyclophane π-prismands is shown clearly in different bonding modes. While in the silver triflate complexes of [2.2.2]cyclophanes bonding is mainly occurring to the "double bonds" of the phenyl rings, the interaction of the silver ion in [2.2.1]-cyclophanes is often found to be above one carbon atom or diffused over many carbons. It appears that [2.2.1]-cyclophanes **1**−**6** are not as suitable for bonding metals as are [2.2.2]cyclophanes **7**−**10**.

The NBO analysis of the present π complexes shows a rather normal bonding back-bonding behavior. The σ-bonding aspect is dominant, although in most cases known in the literature[14,15] the bonding part comes mainly out of the d−π* back-bonding. It appears that when the ligand is able to adapt a suitable orientation, the silver ion bonds preferably between two carbon atoms of the phenyl ring, using a back-bonding mode in addition to the σ -bonding. In cases where the ligand ring size is decreased enough or the phenyl rings cannot adapt to a suitable orientation, the bonding to the Ag^+ ion is accomplished via one carbon instead of a double bond using mainly σ bonding. Thus, it can be assumed that d−π* back-bonding is weaker compared to the σ bonding and occurs only when the ligand conformation is suitable.

Supporting Information Available: Listings of natural charges and Mayer NAO valencies (total atomic bond orders) of all non-hydrogen atoms and overlap-corrected bond orders for Ag^+ and for the atoms surrounding it and counterpoise-corrected calculation energies for π-prismand−silver triflate and π-prismand−Ag^+ complex formation at the HF/3-21G* and the B3LYP/3-21G* levels of theory. This material is available free of charge via the Internet at http://pubs.acs.org.

OM0110134